Spectrochimica Acta Part A: Molecular and Biomolecular Spectroscopy 148 (2015) 338–347

Contents lists available at ScienceDirect

Spectrochimica Acta Part A: Molecular and Biomolecular Spectroscopy

journal homepage: www.elsevier.com/locate/saa

Influence of gamma ray irradiation and annealing temperature on the optical constants and spectral dispersion parameters of metal-free and zinc tetraphenylporphyrin thin films: A comparative study

H.M. Zeyada [a], M. M. Makhlouf [a,b,c,*], M.M. El-Nahass [d]

[a] Department of Physics, Faculty of Science at New Damietta, 34517 New Damietta, Egypt
[b] Department of Physics, Faculty of Applied Medical Sciences at Turabah, Taif University, 21995, Saudi Arabia
[c] Department of Physics, Damietta Cancer Institute, Damietta, Egypt
[d] Department of Physics, Faculty of Education, Ain Shams University, Cairo 11757, Egypt

HIGHLIGHTS

- H_2TPP and ZnTPP thin films were prepared by thermal evaporation technique.
- A comparative study has been done between optical properties of H_2TPP and ZnTPP films.
- Influence of annealing temperature and γ-ray irradiation on the optical constants of H_2TPP and ZnTPP thin films have been reported.

GRAPHICAL ABSTRACT

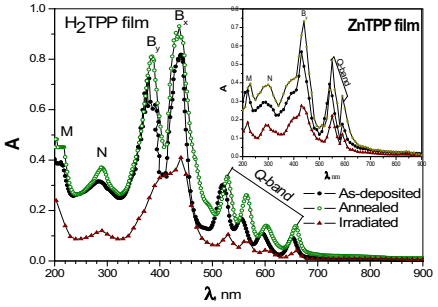

ARTICLE INFO

Article history:
Received 25 August 2014
Received in revised form 2 April 2015
Accepted 4 April 2015
Available online 11 April 2015

Keywords:
Porphyrins
Thin films
Optical properties
Annealing temperature
γ-Ray irradiation

ABSTRACT

In this work, we report on the effect of γ-ray irradiation and annealing temperature on the optical properties of metal-free tetraphenylporphyrin, H_2TPP, and zinc tetraphenylporphyrin, ZnTPP, thin films. Thin films of H_2TPP and ZnTPP were successfully prepared by the thermal evaporation technique. The optical properties of H_2TPP and ZnTPP films were investigated using spectrophotometric measurements of the transmittance and reflectance at normal incidence of light in the wavelength range from 200 to 2500 nm. The absorption spectra of H_2TPP showed four absorption bands, namely the Q, B, N and M bands. The effect of inserting Zn atom into the cavity of porphyrin macrocycle in ZnTPP molecule distorted the Q and B bands, reduced the width of absorption region and influenced the optical constants and dispersion parameters. In all conditions, the type of electron transition is indirect allowed transition. Anomalous dispersion is observed in the absorption region but normal dispersion occurs in the transparent region of spectra. We adopted multi-oscillator model and the single oscillator model to interpret the anomalous and normal dispersion, respectively. We have found that the annealing temperature has mostly the opposite effect of γ-ray irradiation on absorption and dispersion characteristics of these films.

Introduction

Applications of porphyrins are not only limited to biological systems, but also to other fields of science and technology. The technological applications of porphyrins and their derivatives

* Corresponding author at: Department of Physics, Faculty of Applied Medical Sciences at Turabah, Taif University, Saudi Arabia. Tel.: +20 1225486682, +966 533776359; fax: +20 572403868.
E-mail address: m_makhlof@hotmail.com (M. M. Makhlouf).

http://dx.doi.org/10.1016/j.saa.2015.04.008
1386-1425/

include: γ-ray and gas sensors [1,2], solar cells [3], photochromic recording media [4], photonic devices [5], catalysis [6] and photo-electrochemical cells [7]. Porphyrins also show relatively high efficiencies in the dye-sensitized solar cells (DSSCs) [8,9]. Porphyrins have been regarded as promising dye sensitizers in DSSCs due to their good absorption properties and synthetic versatility. Active efforts in the modifications of porphyrin molecules have recently led to a reasonable power conversion efficiency exceeding 13% in an optimized DSSC [10].

Porphyrins are a conjugated organic macrocycles consisting of four pyrrole-derived units (C_4H_4NH) fused together through the bridging carbon atoms. The porphyrin skeleton has an extended π-conjugation system with 18-π electrons leading to a wide range of wavelengths for light absorption; this can also be tuned by attaching different functional groups to the porphyrin ring [11,12]. Linker groups can be attached to different parts of the molecule for binding it to the surface [11,12]. This may be done as well by choosing proper central metal atoms [11–13]. These molecules play an important role for the life of plants; they are a central light-absorbing unit in the chlorophyll II molecule, as well as the life of animals and humans, as a main part of the hemoglobin molecule, the red blood cell pigment responsible for transport of oxygen and CO_2 in the blood [14,15]. Most of porphyrins often form so-called H-aggregates, where the neighboring molecules are stacked with their macrocycles "face-to-face" [16–18]. The physicochemical functions and spectroscopic properties of porphyrins and metalloporphyrins are related to the group and position of substituent at the porphyrin macrocycles. Therefore, the synthesis, structure and spectroscopic properties of porphyrins and metalloporphyrins continue to be an active and productive area [19,20].

Porphyrins have been used for the photosensitization of metal oxides, the most common of them are the metal-free tetraphenylporphyrin, H_2TPP, and zinc tetraphenylporphyrin, ZnTPP, they are also occupy the central interest to the study presented in this paper. These molecules consist of a central porphyrin ring and four phenyl (C_6H_5) rings attached to it through four C–C bonds, as shown in Fig. 1(a). As the Zn atom is introduced into the cavity of the H_2TPP molecule and bounded by four nitrogen atoms during the metalation process, the molecule becomes the zinc tetraphenylporphyrin, ZnTPP, as shown in Fig. 1(b). Due to the steric interaction between the hydrogen atoms on the porphyrin ring and phenyl rings, these rings are oriented nearly perpendicular to one another which decreases the overlap of the π-orbital located on these two parts of the molecule and consequently makes them almost completely electronically decoupled [21].

The absorption spectra of H_2TPP and ZnTPP films showed different bands depending on the method of its preparation [22,23]. The absorption spectra of H_2TPP in nematic liquid crystals have been studied [23]; the spectrum showed characteristic Soret band in the visible region 400–500 nm and four small bands in the Q-band region 500–650 nm. Harime et al. [23] obtained similar absorption spectra for H_2TPP dissolved in chloroform solvents.

The influence of temperature changes on the thermal and structural behavior of crystalline solvates of H_2TPP with 1,4-dioxane and of CuTPP with benzene were investigated using X-ray diffraction, thermogravimetry and differential scanning calorimetry techniques [24]. X-ray diffraction measurements showed that desolation in benzene caused a minor decrease in the volume of the unit cell containing the same number of CuTPP molecules. The symmetry of the crystalline lattice changed from monoclinic to triclinic crystal system. There is a reversible thermal effect for crystals of H_2TPP obtained both by sublimation and by crystallization from 1,4-dioxane.

The exposure of solid materials to ionizing radiations such as γ or X-rays irradiation produce changes in the microstructural

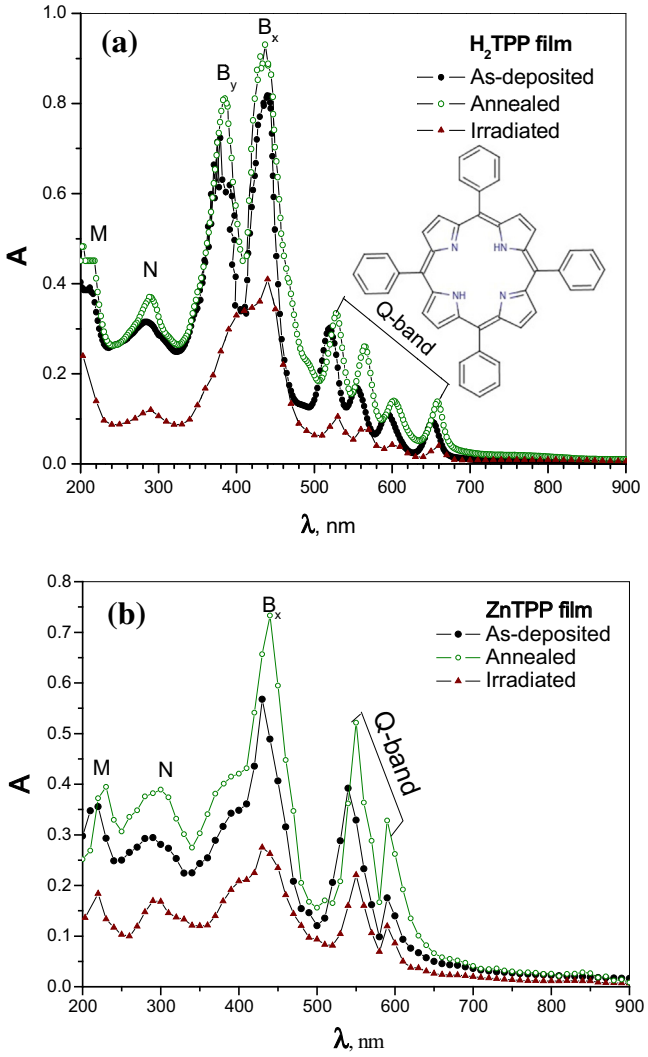

Fig. 1. Absorption spectra, *A*, as a function of wavelength, λ, for, (a) metal-free tetraphenylporphyrin, H_2TPP, and (b) zinc tetraphenylporphyrin, ZnTPP, thin films.

properties of the material as a result of inducing the structural defects, which in turn affect the optical properties. The change in structure depends on the type and dose of irradiation and sensitivity of the solid films to respective irradiation. The influence of γ or X-rays irradiation on the structural and optical properties of some porphyrins derivatives in the form of thin films has been investigated in Refs. [24–29]. The effect of γ-irradiation on the nickel tetraphenylporphyrin, NiTPP, thin film morphology has been investigated by XRD, AFM and TEM for as-deposited and γ-irradiated films [24]. The results show polycrystalline and amorphous nature for as-deposited and γ-irradiated NiTPP films, respectively. The optical properties of NiTPP thin films before and after gamma-irradiation have been investigated by means of spectrophotometric measurement. It is found that the energy band gap of 1.93 eV for as-deposited films, γ radiation decreased it to 1.65 eV. In addition, γ-irradiation affects the values of the calculated dispersion parameters such as oscillator energy, dispersion energy and dielectric constant. γ-Irradiation with doses up to 20 kGy decreases the refractive index, *n*, and extinction coefficient, *k*, of the iron(III) chloride tetraphenylphorphyrin, FeTPPCl [25]. The optical properties of 5,10,15,20-tetrakis (4-methoxyphenyl)-21*H*,23*H*-porphine cobalt(II), CoMTPP thin films before and after irradiation have been studied in the spectral range 200–2500 nm and showed the energy

band gap increases with the increase in irradiation dose [26]. Exposing manganese phthalocyanine, MnPc, thick films to γ-ray irradiation changed the electronic transition from direct allowed (for unexposed film) to indirect allowed (for irradiated films) and decreased the optical energy gap with the increase in irradiation dose [27]. Both of absorbance and capacitance of MnPc thick films displayed a highly consistent linear response to γ-ray exposure [27]. The refractive and absorption indices of the cobalt phthalocyanine, CoPc, films increase and energy gap decreases upon their exposure of γ-ray [28]. The molar extinction coefficient and optical energy gap of pyronine thin films decrease by exposing films to γ-rays of 150 kGy [29].

Zewail et al. [30] studied the ultrafast relaxation processes for H_2TPP dissolved in benzene solution at room temperature, where they used fluorescence up-conversion and transient absorption techniques. From the experimental data they inferred an immediate rise (<100 fs) of the Q_x fluorescence upon excitation into Soret and Q_y bands. The analysis of the transient signals led to the conclusion that the electronic relaxation from these electronic states can be described by three time constants: (a) 100–200 fs is assigned to intra-molecular vibration energy redistribution (IVR); (b) 1.4 ps is attributed to vibration redistribution due to elastic collision with solvent molecules and (c) 10–20 ps is required for thermal equilibrium. In another work by Kim and co-workers [31], measurements of the lifetime of the Soret band yielded 68 ± 15 fs. Interestingly, for the gas phase the corresponding lifetime has been estimated to be about 5 ps [31].

Application of H_2TPP and its metal derivatives in photovoltaic devices fabrication is always provided as thin films. To obtain high efficiency and optimize performance of these devices, it is necessary to synthesis a perfect macrocycles of porphyrin derivatives and to control the processing parameters of thin films. In this work, we report on the influence of introducing Zn atom in the cavity of porphyrin ring on the absorption and dispersion characteristics of thermally evaporated H_2TPP thin films, as well as the effect of the annealing temperature and γ-ray irradiation dose on the optical properties of H_2TPP and ZnTPP thin films as a comparative study.

Experimental details

Preparation of thin films

H_2TPP and ZnTPP were purchased from Sigma–Aldrich Chemicals Co., and they were used in a powder form without any further purification. Thin films of H_2TPP and ZnTPP were sublimated by conventional thermal evaporation technique using high vacuum coating system (Model 306A, Edward Co., England). The films were deposited onto clean optical flat quartz substrates for optical measurements; the quartz substrates were carefully cleaned by chromic acid for 15 min and then rinsed by deionized water. The material was sublimated from a quartz crucible source heated by a tungsten coil in a vacuum pressure of 10^{-5} mbar. The rate of deposition was 1.5 nm/s and the film thickness was controlled during evaporation by using a quartz crystal thickness monitor (Model FTM4, Edward Co., England). A shutter, fixed near to the substrate was used to avoid any probable contamination on the substrates in the initial stage of evaporation process and to control the thickness of films accurately.

Experimental techniques

The transmittance, $T(\lambda)$, and reflectance, $R(\lambda)$, spectra of both H_2TPP and ZnTPP thin films were measured at normal incidence of light in the spectral range 200–2500 nm using a double-beam spectrophotometer (JASCO model V-570 UV–VIS-NIR), an uncertainty of 1% was given by the manufacturer for the measurements obtained by this spectrophotometer. The as-deposited films have a thickness of 460 nm. A quartz blank substrate, identical to that one used for the thin film deposition, was used as a reference for the absorption scan. These measurements were also performed for films after being annealed at 473 K with soaking time of 2 h and after being exposed to γ-ray radiation with a dose of 10 kGy generated from a Technetium-99 m generator (Bristol-Myers Squibb Pharma Belgium S.A.).

The model for calculating optical constants

The model used in the present calculations includes a monochromatic beam of light impinging on a thin film deposited on a thick transparent substrate causing multiple reflections to occur at the interface of the system. Assuming that these reflections are coherent inside the thin film and incoherent in the substrate; the absolute expressions of total measured transmittance, T, and reflectance, R, after introducing corrections resulting from absorption and reflection of the substrate, are given by [32–34] as:

$$T_{\text{exp.}} = T_{\text{meas.}}(1 - R_q) \tag{1}$$

where $T_{\text{meas.}}$ is the measured value of transmittance of the film, R_q is the reflectance of reference quartz substrate and

$$R_{\text{exp.}} = R_{\text{meas.}}R_m\left[(1 - R_q)^2 + 1\right] - T^2R_q \tag{2}$$

where $R_{\text{meas.}}$ and R_m are the measured values of the reflectance of the film and the reference Al mirror, respectively.

The refractive index, n, and the absorption coefficient, α, of thin films deposited onto thick non-absorbing substrates can be calculated by using the following equations, respectively [32,34]:

$$n = \left(\frac{4R}{(1-R)^2} - k^2\right)^{1/2} + \left(\frac{1+R}{1-R}\right) \tag{3}$$

$$\alpha = \left(\frac{1}{d}\right)\ln\left[\left(\frac{(1-R)^2}{2T}\right) + \left(\left(\frac{(1-R)^4}{4T^2}\right) + R^2\right)^{1/2}\right] \tag{4}$$

where k and d are absorption index and film thickness, respectively. A computer program [33,35] is used to minimize, simultaneously, the difference between the calculated and the experimental values of both transmittance and reflectance as:

$$|\Delta T|^2 = \left|T_{(n,k)} - T_{\text{exp.}}\right|^2 \tag{5}$$

and

$$|\Delta R|^2 = \left|R_{(n,k)} - R_{\text{exp.}}\right|^2 \tag{6}$$

where $T_{(n,k)}$ and $R_{(n,k)}$ are the calculated values of the transmittance and reflectance using Murmann's exact equations [36,37]. $T_{exp.}$ and $R_{exp.}$ are the experimental absolute values measured from (1) and (2), respectively. By applying the technique adopted in [33,35], unique values of n and k are obtained within the desired accuracy. The experimental errors are taken into account as follows: ±1% for T and R calculations, ±3% for refractive index and ±2.5% for film thickness measurements [38].

Results and discussion

Spectral distribution of absorbance of H_2TPP and ZnTPP thin films

Fig. 1(a and b) shows UV–visible absorption spectra of H_2TPP and ZnTPP for the as-deposited, annealed and γ-ray irradiated thin films, respectively. The spectra consist of two bands, a higher

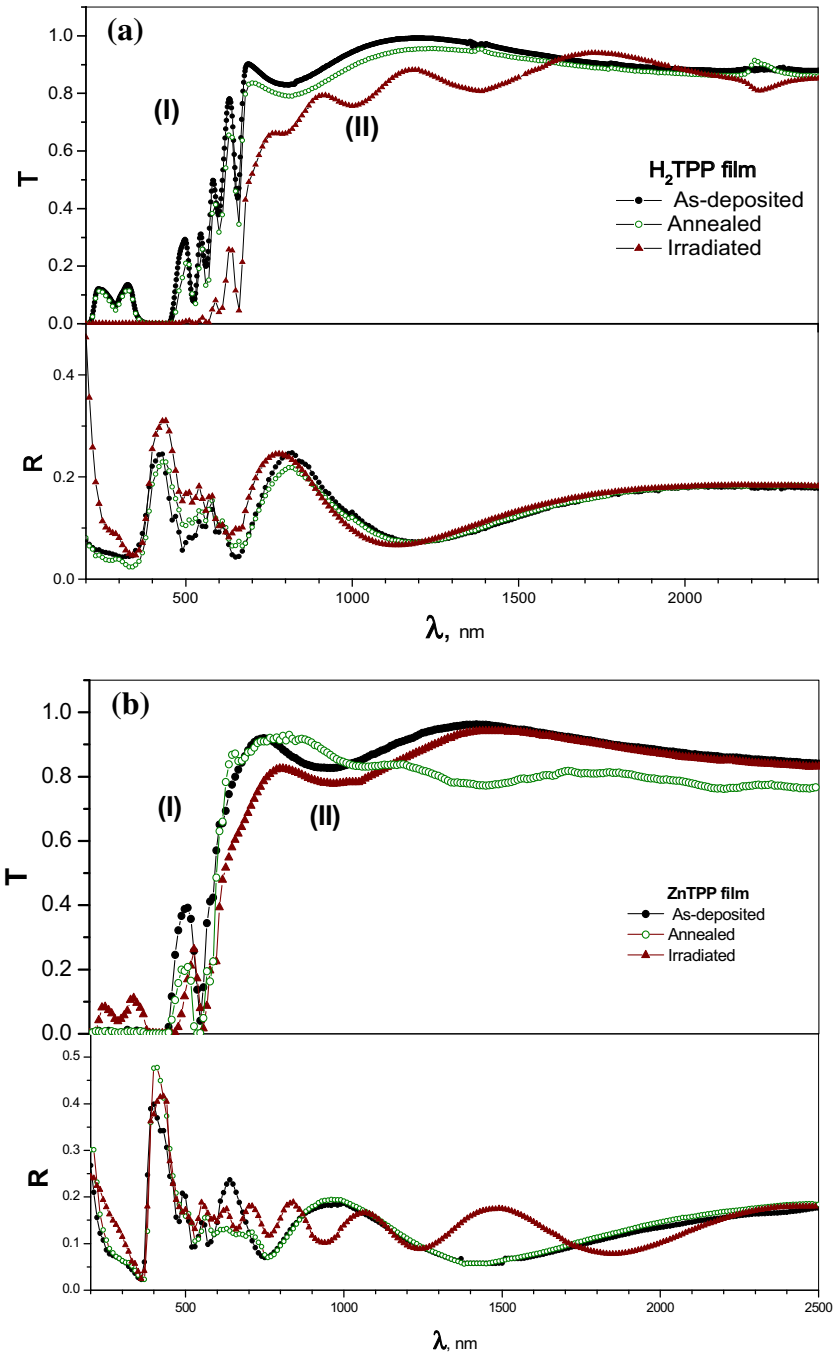

Fig. 2. Spectral distribution of transmittance and reflectance, (a) H_2TPP and (b) ZnTPP thin films in as-deposited, annealed at 437 K and γ-irradiated with a dose of 10 kGy conditions.

energy (shorter wavelength) intense B band, also called Soret band, and lower energy (longer wavelength) weak Q band. The highly conjugated H_2TPP macrocycle shows intense absorption, as shown in Fig. 1(a), termed Soret band, B, that appeared in the wavelength range 335–485 nm and four additional weaker absorptions termed Q bands in the range 490 –720 nm. The Soret band corresponds to a strongly allowed transition from ground state to the second excited state ($S_0 \rightarrow S_2$), whereas Q band corresponds to a transition from ground state to the first excites state ($S_0 \rightarrow S_1$) [36]. Two other bands labeled N and M appear in UV region. The Soret band has two peaks (Davydov splitting [37]), B_x and B_y, at 437 and 385 nm; this splitting depends on the distance between the molecules, the angle of the transition dipole moments with the aggregate, the angle of their transition dipole moments between neighboring molecules and the number of the interacting molecules [33].

Since porphyrin molecules do not contain alone pairs of electrons, both B and Q bands in the UV–visible spectrum are assigned to $\pi \rightarrow \pi^*$ singlet transitions. Metallated porphyrins result in metalloporphyrins such as ZnTPP are more symmetrical, resulting in fewer Q bands and a simpler spectrum. The Soret Band that appeared in the wavelength range 340–490 nm is the highest peak in the UV–vis spectrum, and the Q bands are the smaller bands in the spectrum around 500–650 nm. ZnTPP has Q band consists of two peaks denoted as Q(0,1) and Q(0,0). The main difference between the absorption spectra of ZnTPP and H_2TPP molecules is

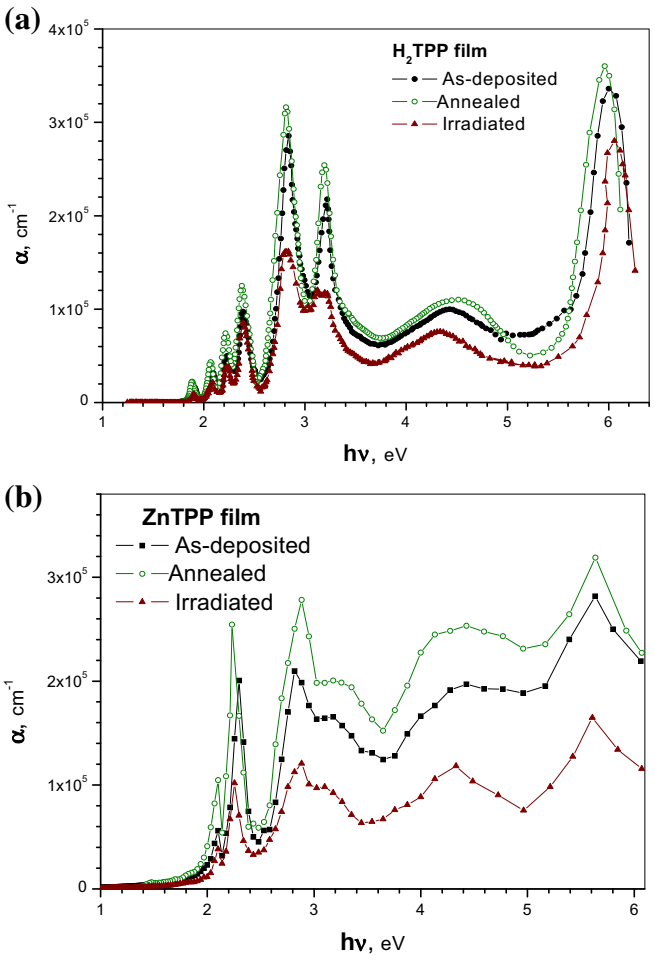

Fig. 3. Spectral behavior of the absorption coefficient as a function of photon energy, (a) H_2TPP and (b) ZnTPP thin films thin films in as-deposited, annealed at 437 K and γ-irradiated with a dose of 10 kGy conditions.

in number of peaks in the Q band. The Q band of ZnTPP consists of two, whereas Q band of H_2TPP consists of four peaks, denoted by $Q_x(0,0)$, $Q_y(0,0)$, $Q_x(0,1)$ and $Q_y(0,1)$ in the spectrum. The Q bands spectra of metalloporphyrins, like ZnTPP, were reduced to two bands in the visible region [36]. The lower energy Q(0,0) band is a result of the excitation to the first excited state, whereas the higher energy Q(1,0) band is often referred to the transition into the higher vibronic state of the macrocycles [36]. Zn metal with a closed electron shell has effect on the absorption spectra of chromophores, due to a small perturbation of the π electrons of the porphyrin ring. Metal orbitals of open shell metals mix much more strongly with the ring orbitals of the porphyrins, that result in more pronounced effect on the absorption spectra, with more intense and fewer of Q-bands, compared to the free base analogue [38].

Annealing of H_2TPP films at 438 K for 2 h results in increases the value of the absorption all over the spectra and a significant broadening of the Soret band and a slightly red shift of Q-bands indicating increased π-conjugation due to increased planarity of TPP molecules [45]. Annealing of ZnTPP film at 438 K for 2 h increases the value of the absorption spectrum, shifts the main peak position of the Q band to longer wavelength side (red shift), such a shift will result in decreasing the energy band gap, whereas exposing H_2TPP and ZnTPP films to γ-ray irradiation reduces the value of absorbance over all the spectra and influences peaks position in comparison with absorbance of as deposited and annealed ones. Increasing irradiation dose decreases amplitude of Q and B bands and shifts the peak positions to shorter wavelength side (blue shift), such a shift will result in increasing the energy gap as shown in Table 2. The exposure of H_2TPP and ZnTPP thin film to ionizing radiations such as γ-ray irradiation generates changes in the microstructural properties of the material as a result of inducing the structural defects, which in turn affect the optical properties. These changes are strongly depending on the internal structure of the material, the radiation energy and the irradiation dose. During γ-ray irradiation, the defects are created within the thin film. At the same time, the defects also get annihilated even under the normal room temperature conditions [39,40]. This creation and annihilation of defects coexist together and at higher doses of γ-ray irradiation, the number of defects created due to γ-ray irradiation equals the number of defects annihilated [40].

The spectral distribution of transmittance and reflectance of films

Fig. 2(a and b) presents the spectral behavior of $T(\lambda)$ and $R(\lambda)$ measured at normal incidence of light in the wavelength range from 200 to 2500 nm for the as-deposited H_2TPP and ZnTPP thin films with a thickness of 460 nm. A transmission band in the wavelength range 210–355 nm for the as-deposited H_2TPP film is

Table 1
Calculated spectral parameters: the wavelength at maximum peak, λ_{max}, molar extinction coefficient, ξ_{molar}, electric dipole strength, q^2, and oscillator strength, f, for the as-deposited, annealed and irradiated (a) H_2TPP thin films and (b) ZnTPP thin films.

λ_{max} (nm)			$\xi_{molar}(\nu) \times 10^4$ (mol l^{-1} cm^{-1})			q^2 (Å)^2			$f \times 10^{-2}$		
As-deposited	Annealed	Irradiated	As-deposited	Annealed	Irradiated	As-deposited	Annealed	Irradiated	As-deposited	Annealed	Irradiated
(a)											
209	213	2.8	7.41	8.25	6.13	4.80	6.79	4.64	1.04	1.55	1.01
274	272	270	2.3	2.5	1.7	5.17	7.17	4.89	0.93	1.86	0.89
384	389	382	4.96	5.86	2.7	4.57	5.74	4.21	1.38	1.63	1.62
436	441	429	6.47	7.33	3.69	7.76	10.4	7.31	3.05	3.20	2.99
517	522	512	2.24	2.82	1.89	1.49	2.31	1.34	0.26	0.46	0.23
555	560	552	1.12	1.66	0.76	1.69	1.27	1.42	0.10	0.18	0.07
595	600	591	0.71	1.02	0.51	0.31	0.51	0.27	0.11	0.14	0.04
652	659	649	0.37	0.48	0.26	0.19	0.31	0.09	0.05	0.07	0.02
(b)											
219	218	222	6.37	7.24	3.65	6.98	8.79	2.96	4.84	6.02	3.89
278	280	289	4.39	5.25	2.68	5.80	6.3	2.39	4.2	4.82	3.11
388[sh]	398[sh]	399[sh]	3.82	4.54	2.26	4.28	5.24	2.91	3.45	4.23	2.96
439	430	429	4.71	6.29	2.71	5.72	6.22	2.78	4.20	5.51	2.22
540	555	549	4.5	5.75	0.28	4.71	4.93	1.48	0.25	0.38	0.12
589	590	591	0.13	2.8	0.81	0.98	1.63	0.67	0.08	0.19	0.05

[sh] Refers to the shoulder.

Table 2
Influence of different conditions on the values of the onset and fundamental energy gaps of H_2TPP and ZnTPP films.

Film conditions	H_2TPP Indirect transition		ZnTPP Indirect transition	
	Onset energy gap (eV)	Fundamental energy gap (eV)	Onset energy gap (eV)	Fundamental energy gap (eV)
As-deposited	1.81	2.50	1.89	2.35
Annealed	1.78	2.45	1.84	2.30
Irradiated	1.85	2.65	1.95	2.42

obvious. A faint band is observed in the same wavelength range for ZnTPP film. The transmission edge is in the wavelength range 457–690 nm for H_2TPP and ZnTPP films. We also observe transmission bands superimposed on the transmission edge. The transmission edge divides the spectrum into two transmission regions. Region (I) is in the wavelength range <690 nm. In this region $R(\lambda)$ is greater than $T(\lambda)$ and their total sum is less than unity, therefore the films are considered to be good absorbers of light, and region (II) lies in the wavelength >690 nm where $T(\lambda)$ is greater than $R(\lambda)$ and their total sum is unity. This means that the films are homogenous and light transparent. In this region of spectrum, the value of absorption index is equal to zero and we can calculate the value of refractive index and dispersion parameters for these films.

Annealing temperature and γ-ray irradiation shift the transmission edge to the higher wavelength side and reduce the peak intensity of the interference maxima and minima of the transmittance and reflectance spectra in comparison to those of the as-deposited films. No new transmission or reflection peaks are observed in the spectrum of annealed or γ-ray irradiated films. This indicates that neither γ-ray irradiation dose nor annealing temperature has any change on the transmittance and reflectance properties of H_2TPP films in absorption region of spectra.

Optical constants

Absorption coefficient spectra of the thin films

A typical absorption coefficient spectra of H_2TPP and ZnTPP films in the as-deposited, annealed and γ-ray irradiated conditions are shown in Fig. 3(a and b). Inserting Zn atom into the cavity of

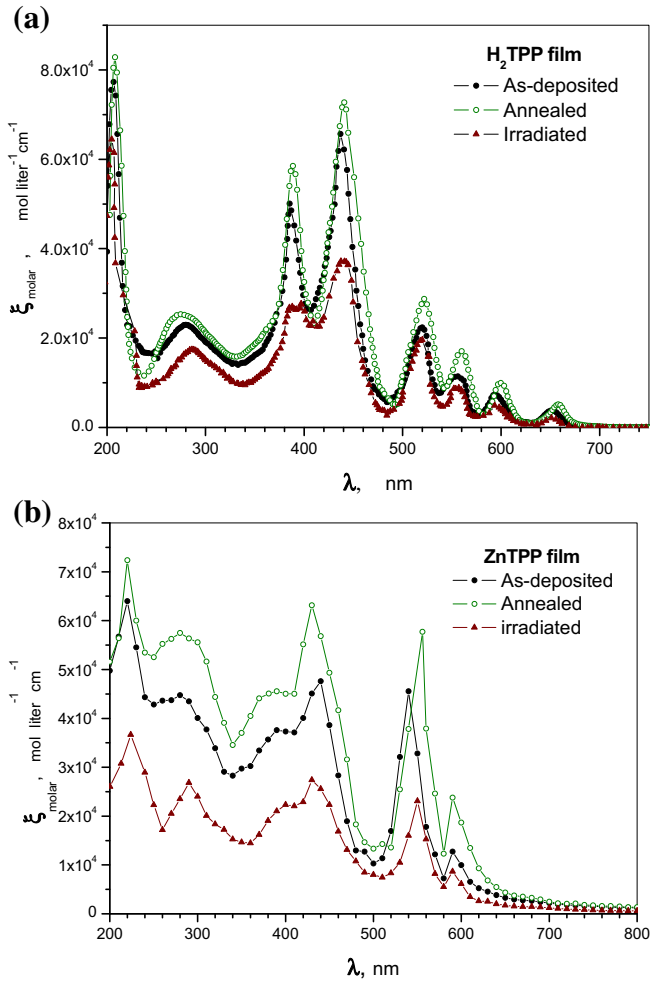

Fig. 4. The spectral behavior of the molar extinction coefficient, (a) H_2TPP and (b) ZnTPP thin films in as-deposited, annealed at 473 K and γ-irradiated with a dose of 10 kGy conditions.

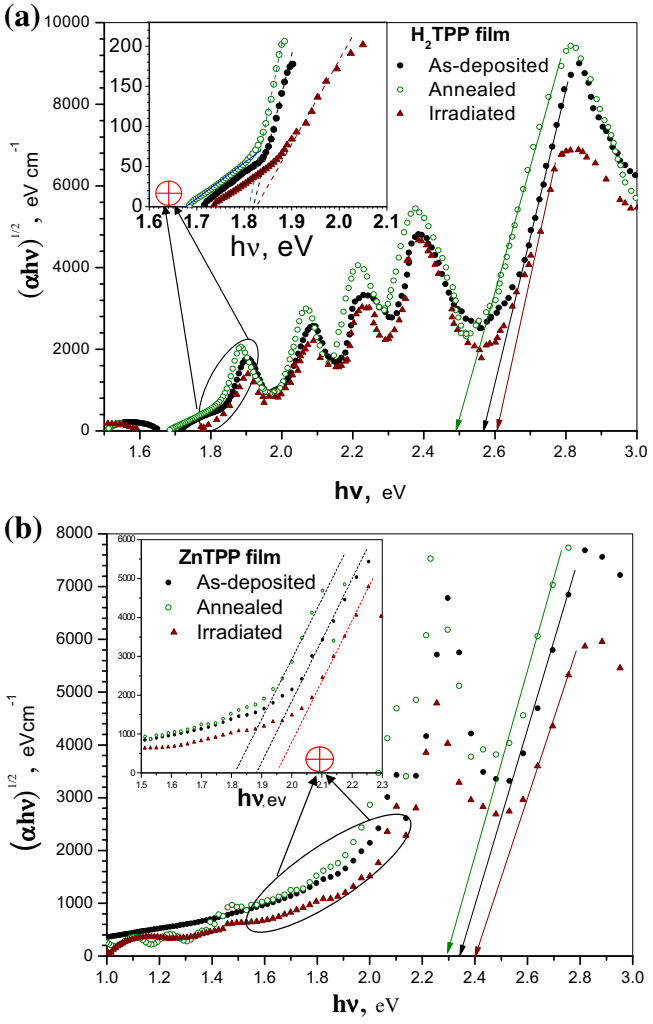

Fig. 5. The relation between $(\alpha h\nu)^{1/2}$ and photon energy, $h\nu$, (a) H_2TPP and (b) ZnTPP thin films in as-deposited, annealed and γ-irradiated thin film conditions.

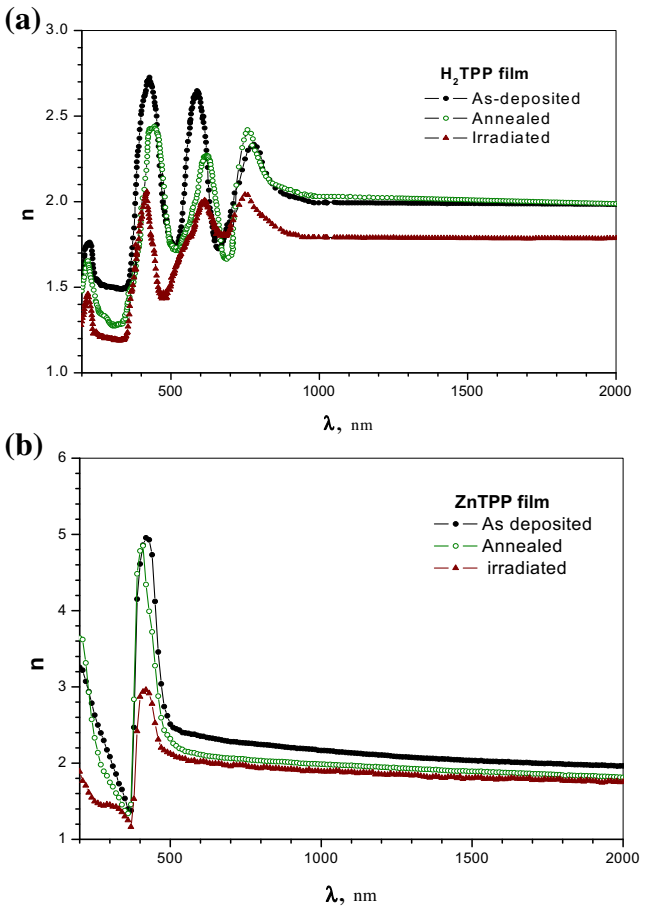

Fig. 6. The dispersion curve of the refractive index $n(\lambda)$, (a) H_2TPP and (b) ZnTPP thin films in as-deposited, annealed at 473 K and γ-irradiated with a dose of 10 kGy conditions.

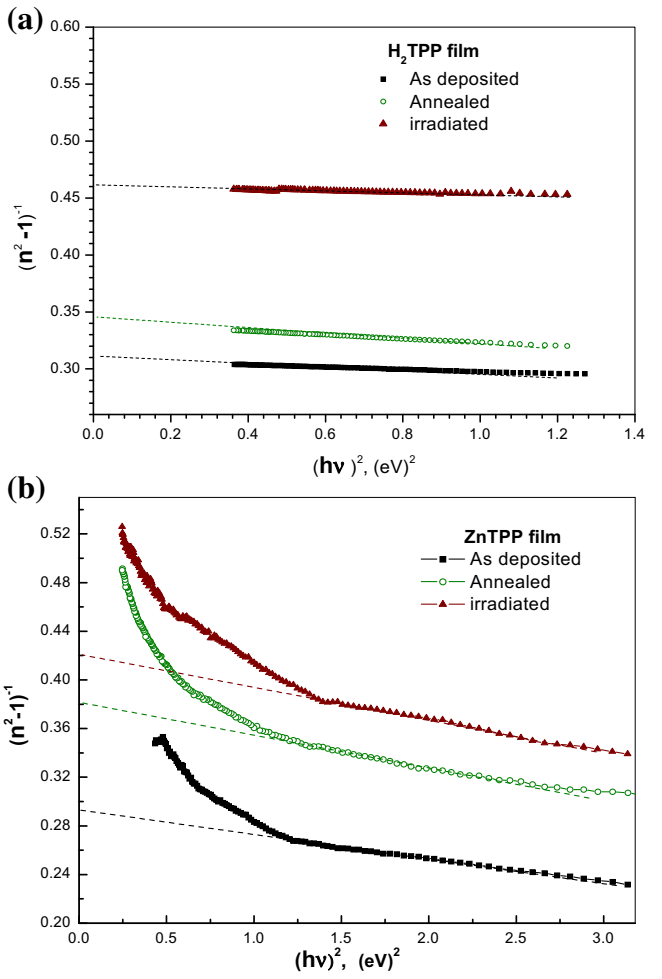

Fig. 7. Plots of $(n^2-1)^{-1}$ versus the squared photon energy $(h\nu)^2$, (a) H_2TPP and (b) ZnTPP thin films in as-deposited, annealed at 473 K and γ-irradiated with a dose of 10 kGy conditions.

H_2TPP macrocycle distorted the Q and B bands, such a behavior has been observed in Ni(II)TPP [24], Fe(III)ClTPP [25] and CoMTPP [26] thin films.

Annealing of H_2TPP and ZnTPP films at 473 K for 2 h increases the value of the absorption coefficient all over the spectra and causes a significant broadening of the Soret band. A slight red shift of Q-bands is observed which indicates increased π-conjugation due to increased planarity of H_2TPP and ZnTPP molecules [45]. Kasha's exciton model [46] interprets the red shift as a case of in-line dipoles transition that occur for the long geometrical axes of the molecule parallel to polarization axes, but with transition dipoles polarized along the short axis of a unit molecule. The magnitude of the red shift is consistent with the decrease in the band gap between the highest occupied molecular orbital (HOMO) and lowest unoccupied molecular orbital (LUMO). Table 1 illustrates the absorption peaks maxima and the shift in the bands resulting from the annealing temperature and γ-ray irradiation.

Exposing H_2TPP and ZnTPP films to γ-ray irradiation reduces the value of absorption coefficient all over the spectra and influences peaks positions in comparison with those of the as-deposited and annealed ones. Irradiation dose decreases the amplitude of Q and B bands and shifts the peak position of those bands to the shorter wavelength side (blue shift). Such a shift would result in increasing the fundamental and onset band gap as shown in Table 2. The blue shift is due to parallel transition dipoles and polarization axis of the molecular electronic transition in a composite molecule [46].

Determination of the molar extinction coefficient for H_2TPP and ZnTPP films

The absorption coefficient spectra of H_2TPP thin films have clear peaks representing Q, B, N and M bands. The multioscillator model [47] can be applied to the data of absorption coefficient spectra to obtain the molar extinction coefficient, $\xi_{molar}(\nu)$, by using (7). The spectral behavior of $\xi_{molar}(\nu)$ of H_2TPP and ZnTPP films is shown in Fig. 4(a and b). The two most important spectral parameters are the oscillator strength, f, and the electric dipole strength, q^2; they can be derived from the molar extinction coefficient spectra. The mathematical expressions that had been used in their estimation are expressed in (8) and (9).

For a solid with density, ρ, and molecular weight M, the absorption coefficient, α, is given by [42]:

$$\alpha = 2303\left(\frac{\rho}{M}\right)\xi_{molar}(\nu_o) = G\xi_{molar}(\nu_o) \tag{7}$$

where G is a constant that depends on the material. The oscillator strength, f and the electric dipole strength, q^2 can be deduced from the spectral distribution of ξ_{molar} using a Gaussian fit [42] and they are given as:

$$f = 4.32\times10^{-9}\int \xi_{molar}(\nu_o)d\nu_o \tag{8}$$

$$q^2 = \frac{1}{2500}\xi_{molar}(\nu_o)\frac{\Delta\lambda}{\lambda_o} \tag{9}$$

where $\Delta\lambda$ is the band width at half maximum of the absorption peak expressed in wavelength and λ_o is the wavelength corresponding to resonant frequency.

The oscillator strength and electric dipole moment for the as-deposited, annealed and γ-ray irradiated H_2TPP and ZnTPP thin films are listed in Table 1(a and b). The absorption transitions in the Q-band region have small oscillator strengths due to the opposite directions of the electric dipoles, and the cancellation of electric dipoles that occurs leading to low intensity in the Q bands. The two absorption transitions, B_x and B_y, are due to splitting in the Soret band and have high intensity. This results in large oscillator strength which is due to parallel electric dipoles [36,41]. Therefore, an increase in the magnitude of spectral parameters is related to an increase in both the intensity and broadening of the absorption band. The annealing process increases the intensity of the absorption bands, as shown in Fig. 4(a and b), due to changing the orientation of some electric dipoles through 180° which, consequently results in changing the oscillator strength. Annealing and γ-ray irradiation influenced the peak positions of molar extinction coefficient for H_2TPP and ZnTPP films, the effect of annealing temperature on these parameters is more pronounced than the effect of γ-ray irradiation.

Determination for energy band gap of H_2TPP and ZnTPP films

The type of the electron transition and the value of the energy gap, E_g, may be determined from the analysis of the absorption coefficient, α, near the optical and the fundamental absorption edge. This can be done by adopting the framework of the one-electron theory [43]. The type of transition and the optical energy gap values for the semiconductors can be obtained by using Tauc's relationship as shown in the following equation [44]:

$$\alpha h\nu = \beta(h\nu - E_g)^r \quad (10)$$

where β is a constant related to the electrical conductivity and energy level separation, $r = 2$ or 3 for indirect allowed and forbidden transitions, respectively and $r = 1/2$ or 3/2 for direct allowed and forbidden transitions, respectively. The dependence of $(\alpha h\nu)^{1/r}$ on photon energy ($h\nu$) for onset and fundamental gaps were discussed and plotted for different values of r. The best fit of the experimental results was obtained for $r = 2$ as illustrated in Fig. 5(a and b). The relation between $(\alpha h\nu)^{1/2}$ and ($h\nu$) for the as-deposited, annealed and γ-ray irradiated films is linear in the region of strong absorption edge for onset and fundamental gaps. The intercept of the straight-line graphs with the abscissa axis gives the values of the optical and fundamental band gaps as shown in Fig. 5(a and b). The values of indirect allowed energy gap, E_g^{ind}, for the as-deposited, annealed and γ-ray irradiated films are listed in Table 2. The fundamental energy gap is the energy gap between HOMO–LUMO bands [33]. The energy levels in between are either traps or impurity energy levels. The calculated energy gap for Q-band between HOMO and LUMO orbitals of H_2TPP is 1.81 eV in good agreement with that reported by Shaffer et al. [45]. It is obvious that the energy gap decreases with increasing the annealing temperature and increases by exposing the film to γ-ray irradiation.

The onset and fundamental energy gaps depend on processing parameters. Incorporation Zn atom into the cavity of H_2TPP molecule increases the optical energy gap and decreases the fundamental energy gap. Annealing temperature has the opposite effect of γ-ray irradiation on optical and fundamental energy gaps of H_2TPP and ZnTPP films. Annealing temperature decreases both of the onset and fundamental energy gaps as shown in Table 2. As a direct consequence of decreasing the energy gap, the absorption coefficient of H_2TPP films increases (Fig. 3(a and b)). The decrease of fundamental energy gap upon annealing has been observed in NiTPP films [46]. The B_y band becomes a shoulder upon

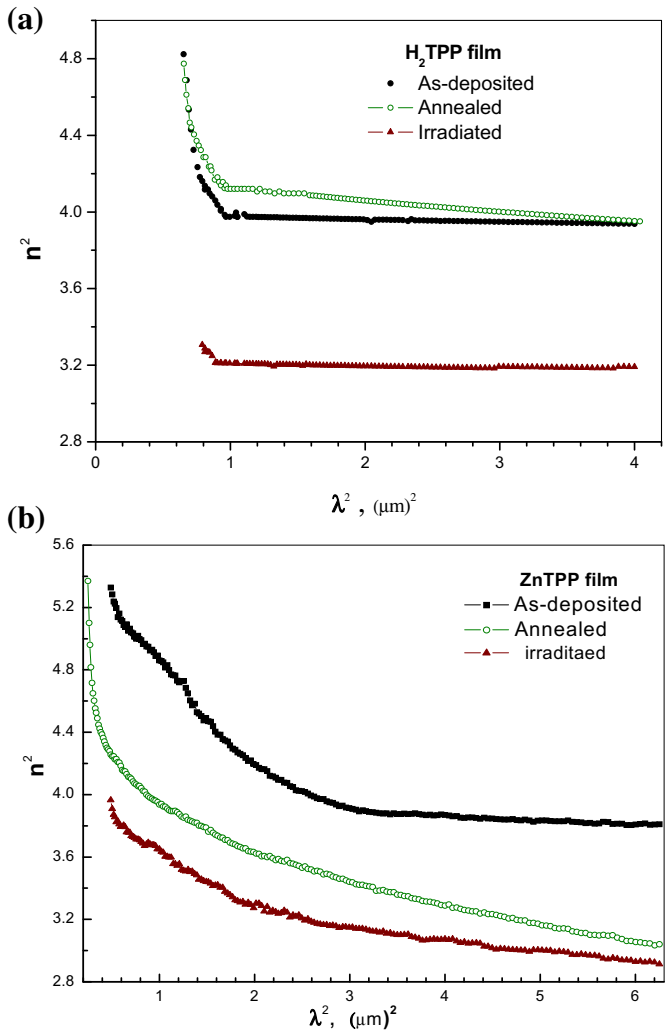

Fig. 8. Plots of squared refractive index, n^2, versus the squared wavelength, λ^2, (a) TPP and (b) ZnTPP thin films in as-deposited, annealed at 473 K and γ-irradiated with a dose of 10 kGy conditions.

exposure to γ-ray irradiation; this indicates that structural disorder and traps are introduced into the band gap upon exposure to γ-ray irradiation. γ-Ray irradiation causes a red shift of the bands resulting in an increase of fundamental energy gap, this results in reducing absorbance all over the spectra. The increase of energy band gap upon γ-ray irradiation has been observed in CoMTPP films [26].

Dispersion characteristics

The spectral distribution of the refractive index

The spectral distribution of the refractive index, n, for H_2TPP and ZnTPP films in the as-deposited, annealed and γ-ray irradiated conditions is illustrated in Fig. 6(a and b). It shows an anomalous dispersion in the range from 200 to 750 nm and exhibits four dispersion peaks for H_2TPP films. The anomalous dispersion is in the wavelength range 200–450 nm with one dispersion peak for ZnTPP; however, a multi-oscillator model [42] can explain the anomalous dispersion.

Incorporating Zn atom in the central cavity of H_2TPP molecule decreases the width and the number of dispersion peaks. It also increases the amplitude of those peaks and refractive index all over the spectra. Annealing and γ-ray irradiation processes shift the

Table 3
Influence of different conditions on the dispersion parameters of H_2TPP and ZnTPP films.

Dispersion parameters	E_o (eV)		E_d (eV)		ε_∞		ε_L		$N/m^* \times 10^{46}$ ($g^{-1}cm^{-3}$)	
Film condition	H_2TPP	ZnTPP	H_2TPP	ZnTPP	H_2TPP	ZnTPP	H_2TPP	ZnTPP	H_2TPP	ZnTPP
As-deposited	5.59	3.57	17.41	12.17	3.96	4.18	4.10	4.13	5.01	7.63
Annealed	5.28	3.43	15.69	11.69	4.11	3.72	3.96	3.89	5.62	4.26
Irradiated	4.98	3.56	11.87	9.45	3.51	3.89	3.23	3.33	17.51	18.20

Table 4
Influence of processing parameters on $\chi^{(3)}$ and n_2.

Thin film	n_2 (10^{-12} esu)			$\chi^{(3)}$ (10^{-13} esu)		
	As-deposited	Annealed	Irradiated	As-deposited	Annealed	Irradiated
TPP	7.14	5.82	2.60	3.77	3.13	1.29
ZnTPP	9.95	10.5	5.87	5.40	5.38	3.07

peaks slightly towards high wavelength values and reduce intensities of dispersion peaks. The results of refractive index, n, depicted in Fig. 6(a and b) show dispersion peaks in UV–visible region, these are attributed to electronic transition across π–π^* orbital [36,41]. Annealing and γ-ray irradiation reduces the value of the refractive index all over the spectra for H_2TPP and ZnTPP thin films. The decrease of the refractive index with annealing temperature and γ-ray irradiation is related to the decrease of mass density of H_2TPP and ZnTPP films, such behavior has been reported in other metallotetraphenylporphyrin thin films [24–26].

Determination of dispersion parameters

In the transparent region of spectra, the spectral dependence of refractive index can be explained by adopting single oscillator model proposed by Wemple and DiDomenico [47], in this model the refractive index is related to the dispersion parameters by:

$$\frac{1}{n^2-1}=\frac{E_o}{E_d}-\frac{1}{E_oE_d}(h\nu)^2 \tag{11}$$

Where $h\nu$ is the photon energy, E_o is the oscillator energy that gives quantitative information on the overall band structure of the material and E_d is the dispersion energy which is a measure of the strength of inter-band optical transition inside the material [48]. A plot of $(n^2-1)^{-1}$ versus $(h\nu)^2$ for H_2TPP and ZnTPP films in the as-deposited, annealed and γ-ray irradiated conditions are illustrated in Fig. 7(a and b). The oscillator energy, E_o, and the dispersion energy, E_d, are directly determined from the slope $(E_oE)^{-1}$ of the linear portion of the curve and its intercept with ordinate axis (E_o/E_d). The intercept of the linear portion of the curve with ordinate axis determines also the value of ε_∞. The values of E_o and E_d decrease by applying processing parameters. E_o and E_d have been reported to be related to the bond length, L, in the way $E_o \propto L^{-s}$ and E_d depends on L^s, with s varying in the range $2 < s < 3$ [49]. The variation of E_o and E_d by processing parameters indicates a change in the bond length of H_2TPP molecule. The lattice dielectric constant, ε_L, and the ratio of carrier concentration to the effective mass, N_c/m^*, in the transmission region of spectra can be also deduced from the relation [26,33]:

$$n^2=\varepsilon_L-\left(\frac{e^2}{4\varepsilon_o\pi^2c^2}\right)\left(\frac{N}{m^*}\right)\cdot\lambda^2 \tag{12}$$

where N/m^* is the ratio of the carrier concentration to the electron effective mass, e is the electron charge and c is the velocity of the light. The graphical representation of n^2 as a function of λ^2 for the as-deposited, annealed and γ-ray irradiated H_2TPP and ZnTPP films is shown in Fig. 8(a and b). By extrapolating the linear part towards the shorter wavelength, the intercept with the vertical axis (at $\lambda^2 = 0$) gives the value of ε_L and from the slopes of these lines the ratio N/m^* can be calculated.

The results of the influence of different conditions on dispersion parameters of H_2TPP and ZnTPP films are listed in Table 3. Annealing and γ-ray irradiation influences the values of dispersion parameters in comparison to those values of as-deposited H_2TPP and ZnTPP film. The value of ε_L differs from the value of ε_∞ and this may be attributed to the free carrier absorption [33]. N/m^* varies with processing parameters and therefore ε_L and ε_∞ depend on the processing conditions. The effect of γ-ray irradiation on those parameters is greater than the effect of annealing temperature.

Nonlinear optical characteristics

The hyperpolarizability values may be used to explain the distortion of the ring caused by processing parameters. Hyperpolarizabilty values are directly proportional to the imaginary component of the third order susceptibility, $I_m(\chi^3)$, [50]. A combination of Miller's generalized rule with linear refractive index and dispersion parameters (E_o and E_d) are used to calculate $I_m(\chi^3)$ by the following relation [50]:

$$I_m(\chi^3)=A_o(E_d/E_o)^4/(4\pi)^4=A_o(n_o^2-1)^4 \tag{13}$$

where A_o is 1.7×10^{-10} (for χ^3 expressed in esu) and n_o is the static refractive index and it can be calculated by using (14) at the limit of n as $h\nu$ approaches zero,

$$n_o=\left(1+\frac{E_d}{E_o}\right)^{1/2},\quad \varepsilon_\infty=n_o^2 \tag{14}$$

The nonlinear refractive index n_2 can be calculated from the relation [50]:

$$n_2^2=12\pi\chi^3/n_o \tag{15}$$

The variation in the values of $I_m(\chi^{(3)})$ and n_2 with processing parameters are listed in Table 4. The increase in the values of $I_m(\chi^{(3)})$ and n_2 with processing parameters indicates that the macrocycle of H_2TPP is greatly influenced by these parameters.

Conclusions

H_2TPP and ZnTPP thin films have been grown successfully on quartz substrates by using thermal evaporation technique. The absorption spectra of H_2TPP consists of Q-band in the visible region, an extremely intense Soret band near to UV region, and two other bands labeled N and M in UV region. Inserting Zn atoms in the cavity of H_2TPP molecule reduced the width of the Sort band

and distorted the Q band. Indirect allowed transition is observed in H_2TPP and ZnTPP films. The onset and fundamental energy gap in H_2TPP film are 1.81 and 2.50 eV, respectively. The onset and fundamental energy gap in ZnTPP film are 1.89 and 2.35 eV, respectively.

Annealing temperature decreased the onset and fundamental energy gaps and dispersion parameters of H_2TPP and ZnTPP thin films, while γ-ray irradiation has the opposite effect of the annealing temperature on the above parameters in H_2TPP and ZnTPP thin films. The imaginary part of the third order nonlinear susceptibility and nonlinear refractive index of H_2TPP and ZnTPP were calculated.

References

[1] P. Muthukumar, S. Abraham John, Sens. Actuat. B Chem. 159 (1) (2011) 238–244.
[2] H.M. Zeyada, M.I. El-Gammal, O.A. ElBatrawy, B.M. Omar, Phys. Scr. 86 (2012) 065801.
[3] M.M. Makhlouf, H.M. Zeyada, Solid State Electron. 105 (2015) 51–57.
[4] J. Durantini, G. Morales, M. Santo, M. Funes, E.N. Durantini, F. Fungo, T. Dittrich, L. Otero, M. Gervaldo, Org. Electron. 13 (4) (2012) 604–614.
[5] D. Wrbel, A. Siejak, P. Siejak, Sol. Energy Mater. Sol. Cells 94 (3) (2010) 492–500.
[6] J. Li, J. Lie, Q. Wang, H. Ju, Electrochim. Acta 83 (2012) 73–77.
[7] K.D. Seo, M.J. Lee, H.M. Song, H.S. Kang, H.K. Kim, Dyes Pigm. 94 (2012) 143–149.
[8] Y. Oyama, Y. Harima, Eur. J. Org. Chem. 16 (2009) 2903–2934.
[9] A. Hagfeldt, G. Boschloo, L. Sun, L. Kloo, H. Pettersson, Chem. Rev. 110 (2010) 6595–6663.
[10] A. Yella, H.W. Lee, H.N. Tsao, C. Yi, A.K. Chandiran, M.K. Nazeeruddin, E.W.G. Diau, C.Y. Yeh, S.M. Zakeeruddin, M. Grätzel, Science 334 (2011) 629–634.
[11] W.M. Campbell, A.K. Burrell, D.L. Officer, K.W. Jolley, Coord. Chem. Rev. 248 (2004) 1363–1379.
[12] J.H. Chou, H.S. Nalwa, M.E. Kosal, N.A. Rakow, K.S. Suslick, The porphyrin Handbook, vol. 6, Academic Press, 2000.
[13] T.N. Lomova, B.D. Berezin, Russ. J. Coord. Chem. 27 (2001) 85–104.
[14] Paavo H. Hynninen, J. Porphyrins Phthalocyanines 16 (2012) 1167–1176.
[15] W.S. Caughey, G.A. Smythe, D.H. O'Keeffe, J.E. Maskasky, M.I. Smith, J. Biol. Chem. 250 (1975) 7602–7622.
[16] J. Rochford, D. Chu, A. Hagfeldt, E. Galoppini, J. Am. Chem. Soc. 129 (2007) 4655–4665.
[17] E. Galoppini, Coord. Chem. Rev. 248 (2004) 1283–1297.
[18] G. Scott, L.A. Harry, Chem. Commun. 16 (1999) 1539–1540.
[19] Y.H. Zhang, D.M. Chen, T.J. He, F.C. Liu, Spectrochim. Acta A 57 (2001) 2599–2605.
[20] I. Kumadaki, A. Ando, M. Omote, J. Flour. Chem. 67 (2001) 109.
[21] P.J. Walsh, K.C. Gordon, D.L. Officer, W.M. Campbell, J. Mol. Struct. Theochem. 759 (2006) 17–24.
[22] D. Wrbel, J. Goc, R.M. Ian, J. Mol. Struct. 450 (1998) 239–246.
[23] Y. Harima, T. Kodaka, P. Price, T. Eguchi, K. Yamashita, Thin Solid Films 307 (1997) 208–214.
[24] M.M. El-Nahass, H.M. Abd El-Khalek, Ahmed M. Nawar, Opt. Commun. 285 (7) (2012) 1872–1881.
[25] M.M. El-Nahass, A.F. El-Deeb, H.S. Metwally, H.E.A. El-Sayed, A.M. Hassanien, Solid State Sci. 12 (4) (2010) 552–557.
[26] M.M. El-Nahass, A.H. Ammar, A.A. Atta, A.A.M. Farag, E.F.M. El-Zaidia, Opt. Commun. 284 (9) (2011) 2259–2263.
[27] A. Arshak, S. Zleetni, K. Arshak, Sensors 2 (2002) 174–184.
[28] M.M. El-Nahass, A.A.M. Farag, A.A. Atta, Synth. Met. 159 (2009) 589–594.
[29] H.S. Soliman, A.M.A. El-Barry, S. Yaghmour, T.S. Al-Solami, J. Alloys Compd. 481 (2009) 390–396.
[30] J.S. Baskin, H.Z. Yu, A.H. Zewail, J. Phys. Chem. A 106 (2002) 9837–9844.
[31] K.Y. Yeon, D. Jeong, S.K. Kim, Chem. Commun. 46 (2010) 5572–5574 (Cambridge U.K.).
[32] A. Alhuthali, M.M. El-Nahass, A.A. Atta, M.M. Abd El-Raheem, Khaled M. Elsabawy, A.M. Hassanien, J. Lumin. 158 (2015) 165–171.
[33] M.M. Makhlouf, A. El-Denglawey, H.M. Zeyada, M.M. El-Nahass, J. Lumin. 147 (2014) 202–208.
[34] O.S. Heavens, in: G. Hass, R. Thus (Eds.), Physics of Thin Films, Academic, New York, 1964.
[35] H.M. Liddeli, Computer-aided Technique for the Design of Multilayer Filters, Hilger, Bristol, 1981.
[36] M. Gouterman, in: D. Dolphin (Ed.), The Porphyrins, vol. 3, New York, Academic Press, 1978, pp. 1–165.
[37] A.S. Davydov, Theory of Molecular Excitons, Plenum Press, New York, 1971.
[38] G.D. Dorough, J.R. Miller, F.M. Huennekens, J. Am. Chem. Soc. 73 (1951) 4315–4320.
[39] S.L. Sharma, T.K. Maity, Bull. Mater. Sci. 34 (2011) 61–69.
[40] Ateyyah M. Al-Baradi, M.M. El-Nahass, M.M. Abd El-Raheem, A.A. Atta, A.M. Hassanien, Radiat. Phys. Chem. 103 (2014) 227–233.
[41] M. Kasha, H.H. Rawls, A. El-bayoumi, Pure Appl. Chem. 11 (34) (1965) 371–392.
[42] M.M. El-Nahass, Tamer E. Youssef, J. Alloys Compd. 503 (2010) 86–91.
[43] E.J. Baerends, G. Ricciard, A. Rosa, S.J. Van Gisbergen, Coord. Chem. Rev. 230 (2002) 5–27.
[44] M.M. El-Nahass, A.A. Atta, M.M. Abd El-Raheem, A.M. Hassanien, J. Alloys Compd. 585 (2014) 1–6.
[45] A.M. Shaffer, M. Gouterman, Theor. Chim. Acta 25 (1972) 62–82.
[46] M. Dongol, M.M. El-Nahass, A. El-Denglawy, A.F. Elhady, A.A. Abuelwafa, Curr. Appl. Phys. 12 (2012) 1178–1184.
[47] S.H. Wemple, M. DiDomenico, Phys. Rev. B 3 (4) (1971) 1338–1351.
[48] I. Solomon, M.P. Schmidt, C. Sénémaud, M.D. Khodja, Phys. Rev. B 38 (1988) 1326.
[49] H. Chen, W.Z. Shen, Eur. Phys. J. B 43 (2005) 503–507.
[50] D. Dini, M. Hanack, in: K.M. Kadish, K.M. Smith, R. Guilard (Eds.), The Porphyrin Handbook; Physical Properties of Phthalocyanine-based Materials, vol. 17, Academic Press, USA, 2003, pp. 22–31.